Microstructural Analysis of Directionally Solidified Materials Obtained via Line-Scan SLS of Si Films

U.J. Chung*, A.B. Limanov, P.C. van der Wilt, A.M. Chitu, and James S. Im
Program in Materials Science and Engineering, Department of Applied Physics and Applied Mathematics, Columbia University, New York, NY, USA

Phone: +1-212-8547861, Fax: +1-212-8549010, E-mail: uc2111@columbia.edu

Abstract
Line-scan SLS of thin Si films permits the attainment of low-defect-density Si films with a directionally solidified microstructure. This paper deals with: (1) identifying and examining the structural defects that are found in the resultant material, (2) how the spatial variations in the type and density of the observed defects may potentially affect the overall uniformity of the resulting devices, and (3) some technical options that may be applied in order to potentially alleviate the situation.

1. Introduction
The structurally heterogeneous nature of polycrystalline Si (poly-Si) films can exert profound influences on defining the character and determining the characteristics of TFTs that are fabricated using the films. For instance, depending on the microstructural details of the films, the effective channel mobilities of poly-Si TFTs can range from being marginally higher than those of the devices that are made using amorphous Si, to being nearly as high as the values associated with the devices that are made using state-of-the-art SOI substrates.

In general, the specific details regarding the presence and spatial distribution of structural defects present in poly-Si TFTs (which are otherwise identical in design, free from contamination, and optimally fabricated) constitute important factors that dictate both the level of performance and the degree of uniformity of the devices. For those poly-Si films obtained via melt-mediated crystallization of amorphous precursor films on glass substrates, such microstructural details are dictated largely by the details associated with the technique utilized to crystallize the films.

Sequential Lateral Solidification (SLS) corresponds to a melt-mediated crystallization method that relies on pulsed-laser-induced rapid melting and solidification to convert amorphous Si films into crystalline Si films with various low-defect-density microstructures on glass or plastic substrates [1]. As has previously been technically defined and experimentally established [1-3], the SLS method builds on iteratively executing the following process-related requirements: (1) inducing complete melting in an irradiated region of the film — so as to subsequently realize controlled super-lateral growth, and (2) repositioning and re-irradiating the film in order to induce seeded epitaxial lateral growth to initiate from the grains that were laterally solidified during the prior pulse.

The SLS method has thus far revealed itself to be an unusually flexible crystallization approach. Numerous efforts have demonstrated over the years that it is possible to utilize several distinct technical and procedural schemes [2-8] to satisfy the above technical requirements and yield in the process a variety of high-performance TFT enabling materials. Examples of SLS-crystallized materials include uniform-and-large grained poly-Si films (e.g., 2-shot microstructure [9]), polycrystalline films with a directionally solidified microstructure, and location-controlled single crystal regions [2].

2. Line-scan SLS
Line-scan SLS corresponds to a particularly simple variation of SLS that belongs to one of several previously demonstrated schemes of performing SLS [3,4-6,10]. In line-scan SLS, a single line beam (which is preferably (1) as long as possible to maximize the effective rate of crystallization, and (2) sufficiently narrow to, among other things, avoid spontaneous nucleation of solids in the middle of the irradiated region) is employed in order to generate materials with a directionally solidified microstructure

or, alternatively, can be utilized in a particularly efficient manner to produce a 2-shot-microstructured films. It is a straightforward process to produce the directionally solidified materials, as doing so simply involves limiting the relative translation distance of the sample with respect to the beam between the pulses, λ_{step}, to be less than the single-pulse-induced lateral-growth length of the grains, l_g (i.e., $\lambda_{step} < l_g$). Making the 2-shot materials via line-scan SLS is a bit more involved as this requires first avoiding any spontaneous nucleation from taking place and then confining the value of λ_{step} to be such that $l_g < \lambda_{step} < 2l_g$.

The directionally solidified Si films obtained via line-scan SLS are well recognized as being an enabling material for realizing high-mobility TFTs [5,11-15]. All of the previously conducted device-related efforts involving the directionally solidified materials obtained via line-scan SLS clearly demonstrate that high mobility TFTs can be obtained (in the range of ~ 300 to greater than 400 cm^2/Vsec for n-channel devices) — when these highly anisotropic materials are optimally oriented with respect to the devices (i.e., when the current flow is parallel to the elongated/growth direction of the grains).

However, it has also been previously found to be the case that the overall uniformity of such high-mobility TFTs fabricated on a directionally solidified film can actually be less than that of otherwise identically prepared TFTs that are made using a "2-shot" SLS film, which has also been crystallized using the line-scan SLS method (reflected in Figure 1) [11]. Although the exact physical reasons for this observation have not been previously established, it is reasonable to presume — based on the technically established points that were alluded in the introductory section of the paper — the microstructural nonuniformity of the directionally solidified Si as being at least a factor of relevance.

We advocate that it can only be technologically beneficial to thoroughly examine the microstructural details of directionally solidified Si films; as doing so should enable one to accurately evaluate and subsequently optimize — as well as appraise the eventual usability of — the material. This subject matter appears to be particularly pertinent to examine at this point in time as uniform TFTs are actively and increasingly being sought in volume-manufacturing of active-matrix OLED displays and advanced SOG AMLCDs, and noteworthy efforts and investments are being channeled into developing manufacturing-worthy line-scan SLS systems [8].

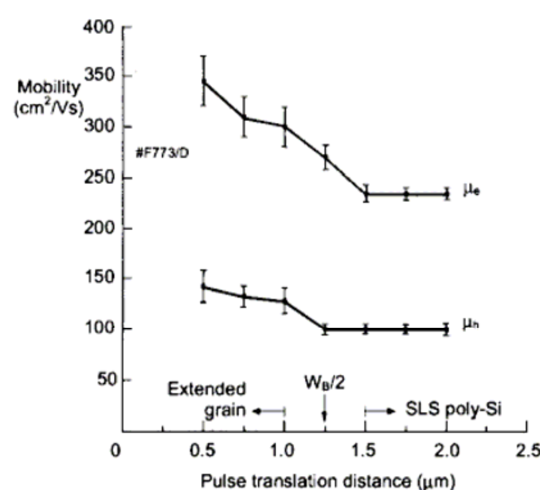

Figure 1 Field effect mobility of TFTs made by line-scan SLS processed Si films ("extended grain" in the figure refers to directionally solidified material, whereas "SLS poly-Si" refers to "2-shot" SLS material) [11].

The present study focuses on investigating the types, characteristics, and concentrations of defects that may be found in the directionally solidified films that are obtained via line-scan SLS of as-deposited amorphous Si films. Even though a certain amount of work has already been done as regards the microstructural analysis of the material [1,6,10,16,17], some potentially critical details, as for instance regarding the presence and prevalence of twin boundaries and stacking faults, remain to be further examined and characterized.

3. Experimental

Our samples consisted of 100-nm-thick amorphous Si (a-Si) films on SiO_2-coated glass substrates. Two SLS systems were utilized in the present study in order to carry out line-scan SLS. The primary SLS system was made up of the following components; an excimer laser (308 nm, XeCl), a pulse duration extender (PDE) capable of elongating the pulse duration up to ~220 ns FWHM (from being initially ~30 ns), a 5× demagnification 2D projection lens system for imaging chromium-on-quartz mask patterns, and a submicron-precision translation stage. Using this system, the samples were line-scan SLS processed with a 500-μm-long and 3.5-μm-wide line beam (without employing the PDE), and at a fixed laser

repetition rate of 10Hz with translation distances (i.e., the "SLS step distance") of 0.5 and 1.0 μm between the pulses.

We have also utilized a 1D-projection-based line-scan SLS system (50 mm beam length) in order to facilitate the preparation of TEM samples [7,10]. The samples processed using this SLS system were irradiated with step distance of 0.70 μm and 2.25 μm, with and without using the pulse-duration extender, respectively.

The microstructural analyses of the defects in the directionally SLS-processed samples were performed using TEM (JEM-100CX) and SEM (JEOL JSM-5600). The samples were moderately and substantially defect-etched for TEM analysis and SEM analysis, respectively. The possible relationship between defect formation and crystallographic-orientation was also explored by analyzing the materials using an EBSD system from HKL.

4. Results and discussion

First and foremost, the overall findings that have been made in the present investigation can be viewed as substantiating the previous findings that have been already reported regarding the microstructure of directionally SLS-processed Si films [1,3,4-6,10,13,16,17]. For instance, it is found that the primary defects that are present in the films are identified as consisting of (1) random high-angle grain boundaries, (2) low-angle grain boundaries, and (3) intragrain and "intrasubgrain" defects consisting primarily of twins and/or stacking faults. (By intrasubgrain defects, we are referring to those defects that are present within the interior of subgrains.) The overall evolution of the microstructure involves, as has been noted previously, occlusion of grains and termination of subgrains, as well as continuous generation and evolution of subgrain boundaries. The orientation analysis of subgrains has revealed that the subgrain boundaries gradually evolve from being initially low-angle grain boundaries often into high-angle grain boundaries as the scan proceeds. Both the generation and evolution of subgrain boundaries appear to be driven by the continual crystallographic twisting of the subgrains, with the axis of rotation mostly parallel to the growth direction of the subgrains. This orientation evolution could very well constitute a fundamental and intrinsic phenomenon, which is generally manifested in all laterally solidified thin films.

The average subgrain width was found to be rather rapidly established as the scan proceeds (in a dynamic manner involving constant generation and convergence of subgrain boundaries) [16,17]. In contrast to this, the average width of the metagrains was found to linearly increase with increasing scan/growth distance. (Here, we introduce and define the term "metagrain" as denoting a crystallized domain that consists of the subgrains that have all originated from one initial seed grain). Consequently, the average number of subgrains within one metagrain is found to also monotonically increase in a linear fashion as a function of the scan distance.

In general, typical subgrains are found to be not entirely free of defects, as they are observed to contain some planar defects. These intrasubgrain defects typically consisted of localized low-angle grain boundaries and twin boundaries that are spatially confined. In comparison to such "normal" subgrains that are generally moderately defective, the following three types of subgrains can be additionally categorized as being microstructurally rather distinctive. These are (I) mostly defect-free subgrains within which a minimal number of structural defects, including low-angle grain boundaries, twins, and stacking faults, are observed within the interior of the subgrains; (II) highly defective subgrains with significant concentrations of feather-like defects (which we presently view as being stacking faults) that tend to crisscross the interior of the subgrains; and (III) highly defective subgrains that contain large amounts of $\Sigma=3$ CSL twin boundaries that run perfectly parallel to each other (i.e., consisting of "twin lamella") and are aligned approximately parallel to the SLS growth direction. TEM micrographs of the three types of subgrains are shown in Figure 2. These pictures were obtained from samples that were lightly chemically defect etched in order to better reveal the presence of defects.

Although microstructurally quite distinct from each other, the type-I and type-II subgrains nevertheless share a number of common characteristics and origins. Specifically, these subgrains: (1) are often found within the same metagrain, which is typically found to be crystallographically oriented with a (100) texture in the direction of the scan (referred to as rolling direction (RD)) and is populated primarily with

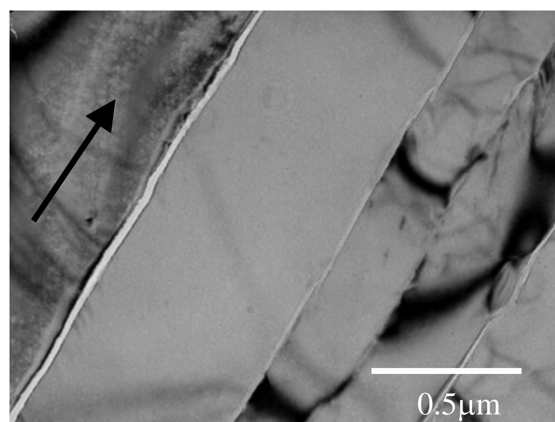

(a)

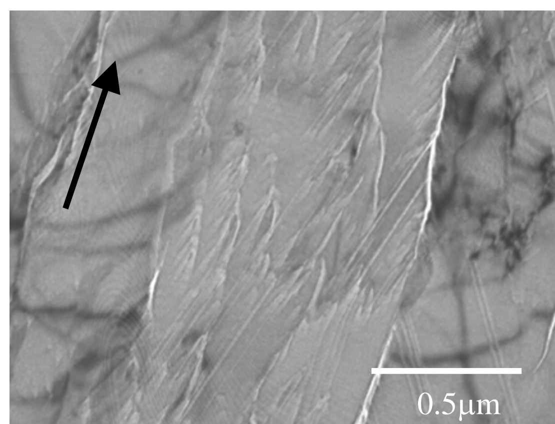

(b)

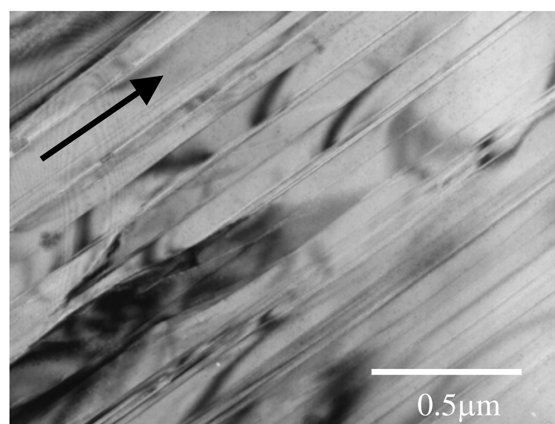

(c)

Figure 2. TEM micrographs showing the three types of atypical subgrains that are observed in directionally SLS-processed 100nm-thick Si films: (a) type-I subgrains that are comparatively free of intrasubgrain defects, (b) highly defective type-II subgrains with feather-like defects, and (c) type-III subgrains that contain numerous twin boundaries. The arrows show the direction of sequential-lateral solidification

normal subgrains that contain moderate and varying amounts of localized planar defects; (2) tend to be often bordered by normal subgrains; (3) typically originate and evolve from normal subgrains; and (4) are not typically sustained over long distances (i.e., mostly short-lived due either to generation of new subgrain boundaries and gradual evolution into normal subgrains (in the case of the defect-free subgrains), and to termination via occlusion by other subgrains and metagrains (in the case of the type-II subgrains)). (We are presently conducting statistically extensive crystallographic orientation analysis of type-I and type-II subgrains as a part of our efforts to identify the fundamental causes that lie behind the formation of these subgrains.)

In general, it may be stated that the type-I and type-II subgrain-populated areas tend to be rather spatially limited, in both widths and lengths. The relative fractions of type I and II subgrains within a (100)-RD textured metagrain are, for the experimental conditions that were explored in the present work, found to be in the range of ~ 10 to 20 %. The typical width of the subgrains is observed to be around one micron or less, and the maximum width (consisting possibly and occasionally of a few subgrains appearing together) is still less than a few microns. Subsequently, these subgrains may end up having a relatively limited impact in terms of dictating the performance characteristics of devices with typical dimensions, since they would occupy only a fraction of the channel area.

In contrast to the type I and II subgrains, the twin-lamella populated type-III subgrains exhibit the following characteristics: (1) they are highly (110)-RD textured; (2) they tend to be surrounded by other type-III subgrains (as, in fact, the majority of subgrains within a (110)-RD textured metagrain tend to be of type-III subgrains [18]); and (3) they are found to be relatively stable as the (110)-RD textured subgrains (and metagrains, as well) are often sustained over long length scales. Consequently the type-III-subgrain populated domains are manifested in a substantially more spatially extended manner, in both widths and lengths.

5. Summary and implications

In the present work, we have experimentally investigated the microstructural uniformity of directionally solidified Si films that are generated via

line-scan SLS. The TEM and SEM analyses of the materials reveal that, in addition to the previously recognized presence of moderately defective subgrains with varying degrees of localized intrasubgrain defects, it is possible to further recognize and categorize the existence of (1) relatively defect-free subgrains (i.e., type-I subgrains), (2) highly defective subgrains containing what appear to be stacking faults (i.e., type-II subgrains), and (3) highly defective subgrains containing twin boundaries that run parallel to each other and are approximately oriented in the scanning direction (i.e., type-III subgrains).

In view of the fact that the type-I and type-II subgrains tend to appear with limited characteristic widths that are smaller than the widths of typically employed TFTs, we deduce that these subgrains would likely have limited influence in terms of degrading the uniformity of conventional TFTs. This could increasingly be the case as one further decreases the thickness of the films (which has been shown to decrease the characteristic subboundary spacing [16]) and increases the width of the devices. Conversely, in the limit of making small-channel-width devices, one may end up producing some very high-performance TFTs and some low-performance TFTs, corresponding respectively to the cases where the devices are placed predominantly on the type-I and type-II subgrains.

In contrast to the spatially confined and localized manner with which the type I and II subgrains typically appear within (100)-RD textured metagrains, the type-III subgrains have been found to appear together in clusters over an entire (110)-RD textured metagrain (which, in turn, may be additionally bordered by other (110)-RD textured metagrains). As the typically observed widths of a type-III subgrain-populated domain can be as large as, or potentially larger than, channel widths of typically employed TFTs, one may presume that the performance characteristics of the resulting devices should be entirely dictated by the intrinsic quality of the material. Consequently, the resulting device characteristics could be rather dissimilar from those that are fabricated on other types of subgrains (i.e., normal, type I, and type II subgrains).

In summary, a reflection on the findings presented in this paper concerning the types and spatial distribution of the defects that can be found in directionally SLS-processed Si films suggests that one fundamental source of nonuniformity can be recognized as the very coexistence of type-III subgrain-containing (110)-RD textured metagrains with other types of subgrains and metagrains. This recognition, in turn, permits one to identify the elimination of such coexistence as an option for possibly improving the uniformity of resulting devices (i.e., the materials consisting entirely of, or entirely devoid of, (110)-RD textured subgrains and metagrains). Fortunately, previous and recent experimental findings reveal that the overall fraction of (110)-RD textured grains can depend in a non-negligible manner on various experimental parameters (e.g., pulse duration, film thickness, step distance, energy density, etc.) [13,18-20]. This dependence does imply that it should be possible to at least improve and optimize the material. Still, more work needs to be done in order to find out whether it would ultimately be feasible to fully eliminate or populate the material with (110)-RD textured subgrains and metagrains.

Alternatively, it may be wise for one to consider the available option of utilizing line-scan SLS to produce 2-shot-microstructured Si films. As shown in Figure 1, doing so has already been demonstrated to lead to substantially more uniform devices, and can be readily and definitively argued as representing a considerably more effective and efficient manufacturing choice. This particular line-scan SLS option can bestow, in addition to providing a mass-production-proven material [9], a number of beneficial processing characteristics in an essentially trivial and penalty-free manner. This includes such production-significant factors as (1) significantly higher throughputs (~3x or greater due to proportionally higher scan speeds), (2) larger effective processing windows (due to enhanced suppression of agglomeration, as a region in the film is irradiated with only one or two pulses), and (3) substantially lower manufacturing and initial investment costs. All that is required at this point is a manufacturing line-scan SLS system capable of executing the 2-shot version of the process.

6. Acknowledgements

This work was supported in part by DARPA-funded AFRL-managed Macroelectronics Program (FA8650-04-C-7101), by Samsung Electronics, Inc. and by Cymer, Inc.

7. References

[1] R.S. Sposili and J.S. Im, *Appl. Phys. Lett.* **69**, 2864 (1996).

[2] J.S. Im, M.A. Crowder, R.S. Sposili, J.P. Leonard, H.J. Kim, J.H. Yoon, V.V. Gupta, H.J. Song, H.S. Cho, *Phys. Stat. Solidi a*, **166**, 603 (1998).

[3] R.S. Sposili and J.S. Im, *Appl. Phys. A* **67**, 273 (1998).

[4] R. Dassow, J. R. Koehler, M. Grauvogl, R.B. Bergmann, and J. H. Werner, *Sol. St. Phen.* **67**, 193 (1999).

[5] R. Dassow, J. Koehler, M. Nerding, H.P. Strunk, Y. Helen, K. Mourgues, O. Bonnaud, T. Mohammed-Brahim, and J.H. Werner, *Proc. MRS* **621**, Q9.3.1 (2000).

[6] A.B. Limanov, V.A Chubarenko, V.M. Borisov, A.Y. Vonokhodov, A.I. Demin, O.B. Khristoforov, A.V. El'tsov, and Y.B. Kiryukhin, *Russ. Microelectron.* **28**, 25 (1999).

[7] J. Shida, presented at *Taiwan FPD International Conference* (2004).

[8] D.S. Knowles, J.Y. Park, C. Im, P. Das, T. Hoffman, P.C. van der Wilt, A.B. Limanov, J.S. Im, *Proc. SID* **36**, 503 (2005).

[9] C.W. Kim, K.C. Moon, H.J. Kim, C.H. Park, I.G. Kim, C.M. Kim, S.Y. Yoo, J.K. Kang, U.J. Chung, *Proc. SID* **35**, 868 (2004).

[10] A. Limanov, and V.M. Borisov, *Proc. MRS* **685E**, D10.1.1 (2001).

[11] S.D. Brotherton, M.A. Crowder, A.B. Limanov, B. Turk, and J.S. Im, *Proc. IDRC* **21**, 387 (2001).

[12] Y.H. Jung, J.M. Yoon, M.S. Yan, W.K. Park, H.S. Soh, H.S. Cho, A.B. Limanov, and J.S. Im, *Proc. MRS* **621**, Q8.3.1 (2000).

[13] A.T. Voutsas, A.B. Limanov, and J.S. Im, *J. Appl. Phys.* **94**, 7445 (2003).

[14] A.T. Voutsas, *IEEE Trans. Electron Devices* **50**, 1494 (2003).

[15] R. Dassow, J. R. Koehler, Y. Helen, K. Mourgues, O. Bonnaud, T. Mohammed-Brahim, and J. H. Werner, *Semicond. Sci. Technol.* **15,** L31 (2000).

[16] M.A. Crowder, A.B. Limanov, and J.S. Im, *Proc. MRS* **621**, Q9.6.1 (2000).

[17] M.A. Crowder, R.S. Sposili, A.B. Limanov, and J.S. Im, *Proc. MRS* **621**, Q9.7.1 (2000).

[18] A.M Chitu, P.C. van der Wilt, U.J. Chung, V.M. McCreary, B.A. Turk, A.B. Limanov, and J.S. Im, these proceedings.

[19] H.S Cho, D.B. Kim, A.B. Limanov, M.A. Crowder, and J.S. Im, *Proc. MRS* **685E**, D11.5.1 (2001).

[20] M. Nerding, S. Christiansen, J. Krinke, R. Dassow, J.R. Köhler, J.H. Werner, and H.P. Strunk, *Thin Solid Films* **383**, 110 (2001).